PHYSICAL REVIEW C

NUCLEAR PHYSICS

THIRD SERIES, VOL. 1, NO. 5 MAY 1970

Elastic Scattering of He^3 by He^4 from 17.8 to 30.0 MeV†

C. G. Jacobs, Jr.,* and Ronald E. Brown
John H. Williams Laboratory of Nuclear Physics, University of Minnesota, Minneapolis, Minnesota 55455
(Received 12 November 1969)

Differential cross sections for the elastic scattering of He^3 by He^4 have been measured from 21.9 to 155.0° (c.m.) at He^3 energies of 17.79, 19.99, 22.00, 23.98, 26.00, 28.00, and 30.00 MeV (lab). The relative standard deviations of the data are typically less than 2.5%, but become larger at angles where the cross section is very low. In addition to relative errors, the over-all error includes a standard deviation of 3% in the cross-section scale. The measurements are compared with theoretical calculations using the resonating-group method in the one-channel approximation. Differences between theory and experiment can be qualitatively understood as being caused mainly by the omission of reaction channels in the theory.

I. INTRODUCTION

Reported here are the results of measurements with the Williams Laboratory MP Tandem Accelerator of differential cross sections for the elastic scattering of He^3 by He^4 in the energy range 17.79 to 30.00 MeV (lab) and a comparison of these measurements with resonating-group calculations for the mass-7 system.[1,2] The present work extends in energy data on He^3+He^4 scattering taken with electrostatic accelerators. In the energy regions of overlap, our differential cross sections are in very good agreement with those of Spiger and Tombrello,[3] but differ significantly from those of Dunnill *et al.*[4] Some data obtained with cyclotron beams exist in the energy range investigated here. We are in definite disagreement with the measurements reported by Bredin *et al.*[5] at 16.6 MeV (c.m.). We are in fair but not complete agreement with Brolley, Stewart, and Rosen,[6] who have commented on the disagreement of their data with those of Chiba *et al.*[7] We also disagree with the data of Chiba *et al.*, especially below a c.m. energy of about 15 MeV. Upon reasonable extrapolation of our measurements to 18.0 MeV (c.m.), we appear to be in agreement with the measurements of Vincent, Boschitz, and Warner.[8] Since the completion of the measurements reported here,[9] other cyclotron data, which overlap ours and extend to higher energy, have been reported.[10-12] These groups have undertaken phase-shift analyses of their data. No phase-shift analysis will be reported here.

In Sec. II a description of the apparatus is given, and in Sec. III the experimental procedure is described and the differential cross sections are presented. Section IV is a short discussion of the resonating-group calculation with which the present data are compared. Also presented is a prediction of a backward-peaked exchange resonance, which would not have been expected to be seen in the present experiment. Indeed, it was not seen. Finally, the comparison of calculation with experiment is discussed in Sec. V, and an experiment is proposed which should observe the predicted exchange resonance.

II. APPARATUS

A. General Facilities

The doubly charged He^3 beam used in this experiment was produced by the MP Tandem Van de Graaff Accelerator at our laboratory. The negative He^3 ions necessary for injection into the main body of the accelerator were made by the passage through lithium vapor of 17-keV, positive He^3 ions extracted from a duoplasmatron source, and the surplus He^3 gas was reclaimed at the output of the source vacuum pump.[13] Negative-ion currents somewhat over 1 μA were readily available if needed. After the doubly charged He^3 beam was pro-

duced by electron stripping in the high-voltage terminal of the accelerator, it was momentum-analyzed, steered, and focused onto a gas cell situated at the center of a 17-in.-diam scattering chamber.[14] This chamber contains independently rotatable upper and lower turntables to each of which was attached a detector assembly. The turntables can be positioned to better than 0.1°. The beam diameter at the gas cell was about 2.0 mm and its angular divergence, which was caused principally by multiple scattering in the cell entrance foil, was about $\frac{1}{3}°$ at the higher energies to about $\frac{1}{2}°$ at the lower energies. After passing through the cell, the beam entered a 178-cm-long 10-cm-diam Faraday cup which contains magnetic electron suppression. Beam-current integration was performed with a system whose charge-collection calibration is known[15] to within 0.5%.

B. Gas-Target System

A cylindrical, 2.5-cm-diam gas cell, covered with 0.0025-mm-thick Havar foil, was used to contain the He^4 gas at the center of the scattering chamber. The cell was connected to a gas-transfer system situated externally to the scattering chamber. Included in the gas-transfer system are a mercury manometer, whose height differential can easily be read to 0.5 mm, and a liquid-nitrogen-cooled trap filled with molecular sieve through which helium can be passed for purification. In the present work, the cell was operated at pressures from 60 to 70 cm Hg.

C. Detector Assemblies

Two detector assemblies were used. One served as a fixed-angle monitor, and the other was used to measure differential cross sections. Detectors were of the solid-state, surface-barrier type with a maximum depletion depth of about 800 μ, and the bias voltages were adjusted to allow protons and deuterons, but not He^3 or He^4 particles, to penetrate through the depletion region. In order to define a limited volume of beam-gas interaction whose reaction products are accessible to a detector, two apertures were placed between each detector and the gas cell. In each detector assembly, the apertures were mounted on the front and back of a tube of 1.9-cm internal diameter, and the solid-state detector was placed directly behind the back aperture. The tube also contained three antiscattering baffles. All detector collimators and baffles were of nickel and were 1.3-mm thick in order to stop energetic protons produced at the higher He^3 energies. The front aperture was a vertical slit and the back aperture was rectangular. The important collimator dimensions were measured with a microscope and calibrated stage.

For the data detector, the front aperture width b was 0.95 mm, the back aperture width was 0.96 mm, the back aperture height was 5.00 mm, the distance h between front and back apertures was 140.0 mm, and the distance R_0 of the back aperture from the scattering-chamber center was 188.7 mm. As has been thoroughly discussed by Silverstein,[16] the geometry factor G which relates counts to cross section may be calculated to high accuracy. To lowest order G is given by

$$G = Ab/R_0h = 1.72\times10^{-5} \text{ cm sr}, \quad (1)$$

where A is the back-aperture area, and the numerical value is for the data detector system. The monitor-system geometry was such that G was equal to 4.32×10^{-5} cm sr. Silverstein[16] has given expressions for corrections to Eq. (1) caused by several effects. For the beam and detector geometries used in the present experiment, all these corrections were negligible.

D. Electronic Apparatus

The signals from the monitor detector were sent to two single-channel pulse-height analyzers. The window of one analyzer was set to encompass the signals produced by both He^3 particles which scatter from He^4 and He^4 recoil particles, and the window of the other analyzer was set to observe any larger signal, which would be produced by He^3 scattering from heavy contaminant nuclei should any be present in the gas cell. The outputs of both analyzers were scaled.

The signals from the data detector were sent into an analog-to-digital converter in which a 256-channel digitization of the signal pulse height was performed. The digital information was then sent to the laboratory Direct Memory Unit,[17] an interface which communicates directly with the memory of a CDC 3100 computer and which was operated so as to allow a 256-channel pulse-height spectrum to be accumulated in a data array in the computer memory. During data accumulation either the data array or a buffer array containing data from the previous run could be manipulated with FORTRAN programs, displayed on an oscilloscope, analyzed with a light pen, and graphed with an automatic plotter.

III. EXPERIMENTAL PROCEDURE AND RESULTS

Differential cross sections were measured at seven He^3 lab energies of 17.79, 19.99, 22.00, 23.98, 26.00, 28.00, and 30.00 MeV. These energies are mean He^3 energies at the center of the gas cell and are known to ±20 keV. The rms energy spread in the beam at the cell center was about 25 keV and was caused principally by straggling in

the Havar foil surrounding the cell. The angular range of the measurements was from 12.5 to about 50° (lab), and at most energies data were taken in steps of 2°. Both scattered He^3 particle and recoil He^4 particles were detected, allowing measurements of differential cross sections from 21.9 to 155° in the c.m. system. The angular resolution of the detection system was about $\frac{1}{3}$° (lab) or $\frac{2}{3}$° (c.m.). In order largely to cancel angular asymmetry effects due to possible beam and detector-collimator misalignment, successive measurements were always made at nominally equal angles on both sides of the incident beam, and the results were averaged. Typically, asymmetries of the order of a few tenths of a degree were observed. The fixed-angle monitor detector was used to keep track of the constancy of important quantities such as target-gas density and beam-current-integrator efficiency. At our typical beam intensities of less than 100 nA, electronic dead-time corrections were of the order of a few tenths of one percent. These corrections were determined by connecting a pulse generator at the preamplifier input and comparing the number of generator pulses recorded in the pulse-height spectrum with the number entering the preamplifier input.

Many tests for accuracy and consistency were performed on the system. Three of the most important of these were: (1) investigation of the effect of beam heating on the gas-cell temperature, (2) investigation of multiple-scattering effects produced when detected particles pass through the Havar foil surrounding the cell, and (3) an over-all check of the system geometry and efficiency by measuring the $H(p,p)H$ differential cross section near 10 MeV. These will now be discussed.

Before data taking was initiated, the helium in the cell was allowed to come to room temperature, and subsequently the gas temperature was taken to be equal to the recorded room temperature. It was therefore important to check that beam densities used in the present experiment would not cause significant heating of the helium gas. A test in which the beam current was varied over a range wider than that used in the present experiment showed no heating effect.

The effect of multiple scattering in the cell on the number of detected particles has been investigated[18] experimentally. This effect is angle dependent both because the scattered He^3 and recoil He^4 energies change with angle and because the influence of the angular shape of the differential cross section depends on lab angle. For example, at some angles, multiple scattering will cause an increase in the number of particles detected; and at other angles it will cause a decrease. Fortunately, in the present experimental situation, the effect is not very large and has been accounted for by suitably increasing the relative errors at low bombarding energies and large lab angles (which correspond to intermediate c.m. angles).

It was decided to test the system by attempting to reproduce the 9.69-MeV (lab), proton-proton scattering data of Johnston and Young.[19] Our differential cross sections were systematically a few percent smaller than theirs. It appears from more recent measurements,[20,21] however, that the cross sections of Johnston and Young may indeed be somewhat too large.

The data were converted to lab differential cross section $\sigma_L(\theta_L)$ by means of the formula

$$\sigma_L(\theta_L) = 0.165\ 84 TzNd \sin\theta_L/(bPQG)\ \text{mb/sr}, \quad (2)$$

where T = target gas temperature in °K, z = charge number per beam particle, N = number of detected particles, d = dead-time correction, θ_L = lab scattering angle, b = number of target nuclei per molecule in the gas cell, P = target gas pressure (cm Hg), Q = beam charge collected (μC), and G = geometry factor (10^{-5} cm sr) as given by Eq. (1). The transformation to c.m. quantities was carried out with fully relativistic formulas.

In Fig. 1 is shown a pulse-height spectrum obtained at 30.00 MeV (lab) and 36° (lab). The pulse-generator peak is not shown. In Fig. 2, graphs of the measured differential cross sections are given. The solid curves are theoretical and will be discussed below. Table I lists the experimental data with relative standard deviations, which include, in addition to statistical errors, relative uncertainties in background subtraction. To obtain the over-all absolute error, an additional error in the cross-section scale of 3% should be added in quadrature to the relative error. The major contribution to

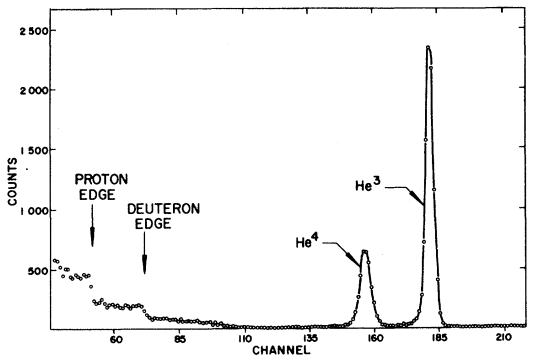

FIG. 1. Pulse-height spectrum at 36° (lab) from the bombardment of He^4 by 30-MeV He^3 particles. The pulse-generator peak is not shown. Evident are peaks due to scattered He^3 particles, recoil He^4 particles, and features due to protons and deuterons which pass through the detector depletion region.

TABLE I. The c.m. differential cross sections and their relative standard deviations, both in mb/sr, for He^3+He^4 elastic scattering. Both the energy in the lab system, in which He^4 is at rest, and in the c.m. system are given. In addition to the relative errors, there is a 3% standard deviation in the absolute cross-section scale.

	Energy (MeV)						
$\theta_{c.m.}$ (deg)	17.79 (lab) 10.14 (c.m.)	19.99 (lab) 11.39 (c.m.)	22.00 (lab) 12.53 (c.m.)	23.98 (lab) 13.66 (c.m.)	26.00 (lab) 14.81 (c.m.)	28.00 (lab) 15.95 (c.m.)	30.00 (lab) 17.09 (c.m.)
21.9	424 ± 13	330 ± 10	311 ± 10	285 ± 9	262 ± 8	261 ± 8	240 ± 8
24.5	332 ± 7	261 ± 6	238 ± 5	...	...	...	...
24.6	...	...	...	224 ± 5	190 ± 4	188 ± 4	164 ± 4
26.3	272 ± 4	...	...	...	...	...	...
28.0	241 ± 3	208 ± 3	175 ± 3	151 ± 2	125 ± 2	112 ± 2	...
28.1	...	...	...	...	...	...	89.7 ± 1.4
31.5	190 ± 2	146 ± 2	124 ± 2	100 ± 2	75.2 ± 0.9	60.4 ± 0.7	43.5 ± 0.5
35.0	146 ± 2	112 ± 2	83.8 ± 0.9	64.0 ± 0.7	41.2 ± 0.5	29.0 ± 0.4	17.8 ± 0.2
38.5	108 ± 2	78.4 ± 0.9	55.0 ± 0.7	37.0 ± 0.5	21.2 ± 0.3	11.5 ± 0.2	6.46 ± 0.10
40.2	92.3 ± 1.0	...	...	...	...	...	...
41.9	84.0 ± 1.2	57.9 ± 1.2	35.0 ± 0.4	19.3 ± 0.4	8.18 ± 0.15	3.42 ± 0.08	...
42.0	...	...	...	...	...	...	2.86 ± 0.06
43.6	72.7 ± 0.8	...	...	...	...	...	...
45.4	62.3 ± 1.0	40.2 ± 0.5	22.7 ± 0.3	10.6 ± 0.1	3.09 ± 0.08	1.11 ± 0.05	2.77 ± 0.07
48.8	51.1 ± 0.6	33.2 ± 0.4	16.6 ± 0.3	7.23 ± 0.24	2.75 ± 0.10	2.54 ± 0.08	4.80 ± 0.09
52.2	45.0 ± 1.5	28.8 ± 0.3	16.3 ± 0.2	9.17 ± 0.15	6.38 ± 0.17	6.57 ± 0.11	8.22 ± 0.11
55.6	40.0 ± 1.0	28.5 ± 0.4	18.4 ± 0.3	13.7 ± 0.4	12.5 ± 0.2	13.3 ± 0.2	...
55.7	...	...	...	...	...	...	13.3 ± 0.2
59.0	40.8 ± 0.5	30.5 ± 0.4	24.2 ± 0.4	22.8 ± 0.3	20.7 ± 0.3	21.4 ± 0.3	20.4 ± 0.3
62.4	38.6 ± 0.5	33.1 ± 0.4	29.1 ± 0.4	29.3 ± 0.8	29.0 ± 0.4	30.6 ± 0.4	28.3 ± 0.4
65.7	39.2 ± 0.5	36.1 ± 0.4	33.9 ± 0.6	36.9 ± 0.5	37.7 ± 0.5	38.8 ± 0.5	...
65.8	...	...	...	...	...	...	36.3 ± 0.5
69.1	37.5 ± 0.9	36.4 ± 0.5	36.6 ± 0.5	41.9 ± 1.0	42.4 ± 0.5	45.2 ± 0.5	42.0 ± 0.5
70.7	36.4 ± 0.9	...	...	...	...	...	...
72.4	33.9 ± 0.8	35.6 ± 0.5	37.1 ± 0.5	43.6 ± 0.5	44.5 ± 0.5	48.4 ± 0.6	45.0 ± 0.5
74.0	31.7 ± 0.8	...	...	...	...	...	...
75.6	28.3 ± 0.9	...	...	...	...	...	...
75.7	...	31.6 ± 0.4	33.9 ± 0.4	39.7 ± 1.4	42.4 ± 0.5	46.1 ± 0.6	44.3 ± 0.6
77.3	25.6 ± 0.7	...	...	...	...	...	...
78.9	22.7 ± 0.6	26.4 ± 0.6	29.7 ± 0.4	35.9 ± 0.5	37.4 ± 0.5	41.3 ± 0.5	...
79.0	...	...	...	...	...	...	40.8 ± 0.5
80.5	20.2 ± 0.5	...	...	...	...	...	...
82.1	17.1 ± 0.5	...	...	...	...	...	...
82.2	...	21.1 ± 0.5	23.5 ± 0.3	28.2 ± 0.5	29.6 ± 0.4	33.1 ± 0.4	32.5 ± 0.4
83.9	13.2 ± 0.6	16.9 ± 0.6	17.8 ± 0.6	21.6 ± 0.7	25.1 ± 0.6	29.4 ± 0.7	27.7 ± 0.4
85.9	11.1 ± 0.5	...	...	...	...	...	...
87.9	8.17 ± 0.33	9.54 ± 0.35	11.3 ± 0.3	13.4 ± 0.4	14.7 ± 0.4	16.7 ± 0.3	17.1 ± 0.3
89.9	5.65 ± 0.26	...	...	...	...	...	...
91.9	4.04 ± 0.20	4.65 ± 0.15	4.90 ± 0.17	6.08 ± 0.19	6.55 ± 0.15	7.58 ± 0.15	7.45 ± 0.16
93.9	2.68 ± 0.16	...	...	...	...	...	...
95.9	1.97 ± 0.13	1.80 ± 0.10	1.82 ± 0.16	2.09 ± 0.08	2.10 ± 0.10	2.18 ± 0.08	2.01 ± 0.10
97.9	1.96 ± 0.10	...	...	...	...	...	...
99.9	2.37 ± 0.12	1.58 ± 0.09	1.50 ± 0.10	1.62 ± 0.07	1.50 ± 0.09	1.47 ± 0.06	1.26 ± 0.07
103.9	4.06 ± 0.13	3.72 ± 0.12	3.77 ± 0.16	4.23 ± 0.12	4.24 ± 0.12	4.67 ± 0.10	4.34 ± 0.10
107.9	6.28 ± 0.19	6.28 ± 0.12	6.64 ± 0.15	7.87 ± 0.21	8.70 ± 0.16	9.86 ± 0.15	9.00 ± 0.16
111.9	7.76 ± 0.31	8.67 ± 0.15	9.53 ± 0.22	11.7 ± 0.2	12.6 ± 0.2	13.8 ± 0.2	13.7 ± 0.2
115.9	8.27 ± 0.16	9.02 ± 0.18	10.3 ± 0.2	12.5 ± 0.4	13.9 ± 0.2	16.3 ± 0.2	15.5 ± 0.2
119.9	7.44 ± 0.26	8.68 ± 0.12	10.1 ± 0.1	10.9 ± 0.2	13.0 ± 0.4	15.2 ± 0.2	15.0 ± 0.2
123.9	5.52 ± 0.12	6.74 ± 0.13	7.66 ± 0.14	8.61 ± 0.24	9.76 ± 0.18	11.7 ± 0.2	11.9 ± 0.2
127.9	4.04 ± 0.19	4.34 ± 0.10	4.97 ± 0.10	5.69 ± 0.09	6.09 ± 0.11	7.37 ± 0.13	7.65 ± 0.12
129.9	3.60 ± 0.08	...	...	...	...	...	...
131.9	2.88 ± 0.17	3.56 ± 0.33	3.39 ± 0.08	3.30 ± 0.13	3.01 ± 0.07	3.62 ± 0.08	4.24 ± 0.07
133.9	4.18 ± 0.18	...	...	...	...	...	...
135.9	5.37 ± 0.14	4.67 ± 0.10	3.34 ± 0.08	2.07 ± 0.06	1.76 ± 0.05	1.43 ± 0.05	1.72 ± 0.04
139.9	9.72 ± 0.29	7.36 ± 0.13	5.33 ± 0.10	3.51 ± 0.07	2.24 ± 0.06	1.40 ± 0.04	1.23 ± 0.04
143.9	16.5 ± 0.4	12.7 ± 0.2	9.77 ± 0.15	6.60 ± 0.11	4.72 ± 0.09	2.83 ± 0.06	1.84 ± 0.05
147.9	26.5 ± 0.4	20.0 ± 0.3	17.0 ± 0.3	11.8 ± 0.3	9.32 ± 0.21	5.58 ± 0.12	3.98 ± 0.11
149.9	31.8 ± 0.5	...	...	...	...	...	...
151.9	40.3 ± 0.9	...	...	...	...	10.0 ± 0.3	8.07 ± 0.21
152.0	...	29.5 ± 0.8	25.1 ± 0.6	18.8 ± 0.4	14.9 ± 0.4	...	...
155.0	51.9 ± 1.6	39.6 ± 1.3	34.0 ± 1.1	24.4 ± 0.8	21.2 ± 0.7	15.1 ± 0.5	12.4 ± 0.4

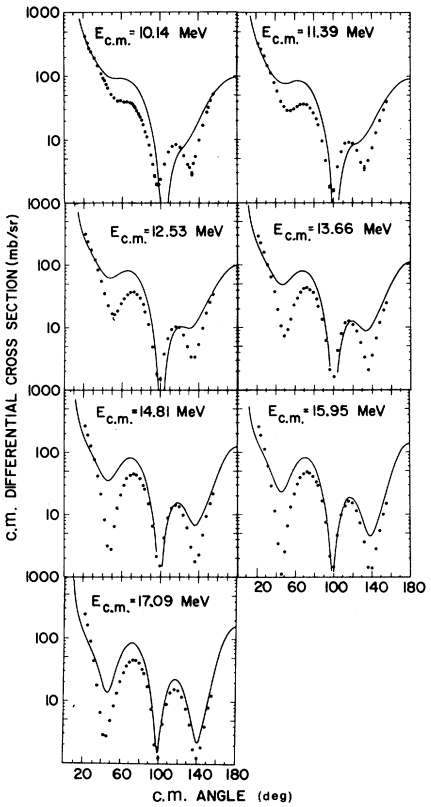

FIG. 2. The c.m. differential cross sections for $He^3 + He^4$ elastic scattering measured in the present work. The solid curves are from the theoretical calculations discussed in Sec. IV.

this scale error is from an uncertainty in extracting the number of counts from the peaks of interest, because the low-energy end of these peaks has a structure caused by scattering and partial penetration effects in the rather thick detector collimators used here.

IV. RESONATING-GROUP CALCULATIONS

Our measured differential cross sections are here compared with the theoretical calculations of Brown and Tang,[1] using the resonating-group method in the one-channel approximation. Briefly, a central nucleon-nucleon potential with exchange terms is employed, and the scattering phase shifts are derived with the aid of a variational principle. In this method, the Pauli principle is taken into account exactly. The calculations presented here include partial waves up to $l=9$, whereas in Ref. 1 only partial waves up to $l=6$ were considered. In spite of the fact that the magnitude of the calculated $l=6$ phase shift for He^3+He^4 scattering is less than 1.1° up to a c.m. energy of at least 22 MeV,[1] the calculation of the differential cross section at the higher energies of the present experiment requires the inclusion of at least the $l=7$ phase shift, which, at these higher energies, actually has a magnitude larger than that for $l=6$. This is because of the l dependence of the effective He^3+He^4 potential pointed out in Ref. 1. The effect on the differential cross sections of the inclusion of partial waves greater than $l=6$ is most readily apparent at angles near 180° and in regions where the cross sections change very rapidly with angle. In Table II are listed the resonating-group phase shifts at the energies of the present experiment and a comparison of the 180° differential cross section with that calculated with only partial waves through $l=6$ included. One notes that at the highest energy a 16% error is made in the 180° differential cross section by truncating the calculation at $l=6$. The error at other angles is generally less than this. The differential cross sections calculated with the phases in Table II are shown as solid curves in Fig. 2, and comparison of these with experiment will be made in Sec. V.

We should mention that, if higher partial waves had been included in Ref. 1, none of the conclusions of that paper would have been changed. Only a graph (Fig. 4 of Ref. 1) which includes a calculated 18-MeV (c.m.) differential cross section would have been modified.

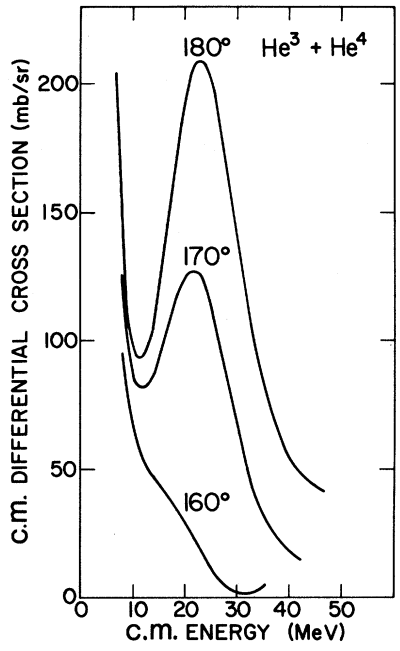

FIG. 3. Backward differential cross sections for $He^3 + He^4$ elastic scattering as a function of c.m. energy, as calculated with the resonating-group method. The energy and angular range of the present experiment would not have allowed observation of the structure presented in this figure.

TABLE II. Phase shifts (deg) up to $l=9$ and 180° c.m. differential cross sections (mb/sr) for He^3+He^4 elastic scattering calculated with the resonating-group method as described in Sec. IV. The last column is the 180° cross section obtained when only phase shifts through $l=6$ are employed. The c.m. energy E is in MeV.

E	$l=0$	1	2	3	4	5	6	7	8	9	$\sigma(180°)$	Truncated
10.14	−96.1	−82.4	−12.2	160.7	−1.90	3.22	−0.34	0.12	0.01	0	97.2	96.4
11.39	−102.3	−88.5	−12.9	161.1	−1.67	4.80	−0.50	0.23	−0.03	0.01	93.5	91.4
12.53	−107.6	−93.7	−13.6	161.3	−1.13	6.55	−0.66	0.36	−0.05	0.01	97.8	93.4
13.66	−112.5	−98.4	−14.4	161.3	−0.28	8.58	−0.81	0.54	−0.08	0.02	107	99.7
14.81	−117.2	−103.0	−15.2	161.3	0.92	10.9	−0.94	0.77	−0.12	0.04	121	109
15.95	−121.6	−107.3	−16.2	161.2	2.43	13.6	−1.03	1.04	−0.16	0.06	137	119
17.09	−125.7	−111.3	−17.2	161.0	4.26	16.5	−1.07	1.36	−0.22	0.10	154	129

In concluding this section we wish to point out an interesting feature of He^3+He^4 scattering predicted by the resonating-group calculation.[22] With the inclusion of partial waves through $l=9$, the differential cross section may be calculated up to about 40 MeV (c.m.). Figure 3 illustrates the calculated differential cross section at 180, 170, and 160° from about 10 to 40 MeV (c.m.). Apparent is a back-angle resonance which is broad in energy but narrow in angular range. It is thought that this is a neutron-exchange resonance, which emerges naturally from the calculation because of the inclusion of exchange forces in the nucleon-nucleon potential and use of a completely antisymmetrized wave function. Unfortunately, the present data extend back to only 155° and up to only 17 MeV (c.m.), and, therefore, we can make no statement as to whether or not such a resonance actually occurs.

V. DISCUSSION AND CONCLUSIONS

Initially, we should stress that no adjustable parameters are used here to obtain fits to the scattering data. Both shape and magnitude of the calculated differential cross sections come from the basic nucleon-nucleon potential and the resonating-group method.

One significant approximation in the calculation[1,2] is the omission of all reaction effects. Figure 2 shows that the calculation gives, in general, too large a cross section, presumably, because of this one-channel approximation. Another feature apparent in Fig. 2 is that the agreement between calculation and experiment of the shape of the differential cross section becomes better as the energy increases. At present it is felt that the poorer agreement in shape at the lower energies is due to the influence of the 9.3-MeV level in Be^7. This level has significant widths for both proton and α-particle emission,[3] and, as Wildermuth and McClure[23] have pointed out, resonances in individual reaction channels can significantly influence the elastic-scattering differential cross section.

Excitation functions plotted (not shown) from the data of Table I do not indicate any clear structure due to possible broad states in Be^7. Indeed, the calculated phase-shift values in Table II indicate that no resonant states having He^3+He^4 structure exist in this energy range. However, to investigate in more detail the level structure of Be^7, a phase-shift analysis using complex phases would be desirable.

Finally, it is suggested that the backward He^3+He^4 scattering cross section be measured up to c.m. energies of 30 to 40 MeV in order to test the resonance prediction illustrated in Fig. 3. When a He^3 particle beam is incident on a He^4 target, the energy of the He^3 particles scattered near 180° (lab) is about $\frac{1}{50}$ of the beam energy. It therefore is somewhat difficult to directly observe the backward-scattered He^3 particles. However, one should be able to observe the He^4 recoil nuclei in the forward direction by allowing both them and the beam to enter a magnetic field, which would then separate the beam from the recoil particles.

ACKNOWLEDGMENTS

We wish to thank the entire technical personnel at the John H. Williams Laboratory for their help throughout the course of this experiment. In particular, we express gratitude to J. Anderson and R. Hendricks for help with mechanical design, D. Varnes for help with mechanical construction, and R. Goodwin for help with computer programming. We are grateful to D. K. Olsen, T. C. Kan, and Dr. J. G. Jenkin for assistance in taking data, and to Dr. Jenkin for several valuable suggestions concerning experimental technique as well. Professor R. K. Hobbie is thanked for many conversations about the efficient use of of our on-line computer. We are grateful to Dr. W. McClure for increasing the number of partial waves in the resonating-group code. Many fruitful discussions about the resonating-group method were had with Professor Y. C. Tang, and to him we express our deep appreciation.

†Work supported in part by the U. S. Atomic Energy Commission.

*Present address: Department of Physics, Pacific Lutheran University, Tacoma, Washington 98447.

[1]R. E. Brown and Y. C. Tang, Phys. Rev. 176, 1235 (1968).

[2]Y. C. Tang, E. Schmid, and K. Wildermuth, Phys. Rev. 131, 2631 (1963).

[3]R. J. Spiger and T. A. Tombrello, Phys. Rev. 163, 964 (1967), and private communication.

[4]F. Dunnill, T. J. Gray, H. T. Fortune, and N. R. Fletcher, Nucl. Phys. A93, 201 (1967), and private communication.

[5]D. J. Bredin, J. B. A. England, D. Evans, J. S. C. McKee, P. V. March, E. M. Mosinger, and W. T. Toner, Proc. Roy. Soc. (London A258, 202 (1960). These. data are also reported by J. S. C. McKee, in Nuclear Forces and the Few-Nucleon Problem, edited by T. C. Griffith and E. A. Power (Pergamon Press, New York, 1960), Vol. II, p. 609. These data were used in Fig. 4 of Ref. 2 to compare with a resonating-group calculation and give the appearance of better agreement with the calculation than do the present data.

[6]J. E. Brolley, Jr., L. Stewart, and L. Rosen, in Nuclear Forces and the Few-Nucleon Problem, edited by T. C. Griffith and E. A. Power (Pergamon Press, New York, 1960), Vol. II, p. 455.

[7]R. Chiba, H. E. Conzett, H. Morinaga, N. Mutsuro, K. Shoda, and M. Kimura, J. Phys. Soc. Japan 16, 1077 (1961).

[8]J. S. Vincent, E. T. Boschitz, and R. E. Warner, Bull. Am. Phys. Soc. 12, 17 (1967). These data are illustrated in Fig. 4 of Ref. 1.

[9]For an earlier report of this work see C. G. Jacobs and R. E. Brown, Bull. Am. Phys. Soc. 12, 1175 (1967). A more detailed discussion is in C. G. Jacobs, Jr., M.S. thesis, University of Minnesota, 1968 (unpublished).

[10]T. A. Cahill and P. C. Martens, Bull. Am. Phys. Soc. 14, 553 (1969).

[11]A. D. Bacher, H. E. Conzett, R. de Swiniarski, H. Meiner, F. G. Resmini, and T. A. Tombrello, Bull. Am. Phys. Soc. 14, 851 (1969).

[12]P. Schwandt, B. W. Ridley, S. Hayakawa, L. Put, and J. J. Kraushaar, Phys. Letters 30B, 30 (1969).

[13]W. D. Harrison and J. G. Jenkin, John H. Williams Laboratory of Nuclear Physics Annual Report, 1968 (unpublished), p. 192.

[14]Oak Ridge Technical Enterprises Corporation, Series 600.

[15]We thank G. J. B. Pyle and A. R. Barnett for making this calibration.

[16]E. A. Silverstein, Nucl. Instr. Methods 4, 53 (1959).

[17]R. K. Hobbie and R. W. Goodwin, Nucl. Instr. Methods 52, 119 (1967).

[18]T. C. Kan, M. S. thesis, University of Minnesota, 1969 (unpublished).

[19]L. H. Johnston and D. E. Young, Phys. Rev. 116, 989 (1959).

[20]R. J. Slobodrian, H. E. Conzett, E. Shield, and W. F. Tivol, Phys. Rev. 174, 1122 (1968).

[21]N. Jarmie, R. E. Brown, R. L. Hutson, and J. L. Detch, Jr., Phys. Rev. Letters 24, 240 (1970).

[22]Y. C. Tang, in Proceedings of the International Conference on Clustering Phenomena in Nuclei, Bochum, Germany, 1969 (International Atomic Energy Agency, Vienna, 1969), p. 109.

[23]K. Wildermuth and W. McClure, in Springer Tracts in Modern Physics, Ergebnisse der exakten Naturwissenschaften, edited by G. Höhler (Springer-Verlag, Berlin, Germany, 1966), Vol. 41.